13th ewtec 2019 Proceedings of the 13th European Wave and Tidal Energy Conference 1-6 Sept 2019, Naples, Italy

Scale model testing of the WASP - a novel wave measuring buoy

Mark Boland, Thomas Kelly, Robert Carolan, Brendan Walsh, Thomas Dooley

Abstract—**To determine the feasibility of sites for proposed wave energy farms, and design optimal wave energy converters, and the most advantageous wave farm arrangements, developers will require knowledge of local wave regimes. Furthermore, local authorities have and increasing need for location specific wave regimes in order to effectively implement coastal protection measures. Wave conditions at a point may be measured using existing buoys, however such devices are expensive, making their use cost prohibitive on many projects. The Wave Activated Sensor Power Buoy (WASP) is a proposed, low-cost wave powered device currently under development. The WASP comprises a floating body with a central moonpool, and uses measurements of the pressure of the air above the water column to estimate the incident wave spectrum. In order to investigate if the spectrum contained within a polychromatic wave may be determined from the variation of air pressure in the chamber of the moonpool of a floating buoy, a testing campaign was conducted on a 1:20 scale model of the JFC Seagull buoy in a wave flume. It is intended that the full-scale WASP be powered using a generator connected to a pneumatic turbine driven by the air flows generated by the motion of the central moonpool in the manner of an oscillating water column device. However, for practical reasons, the central chamber of the 1:20 scale model is sealed. This paper describes the creation, testing and calibration of the 1:20 scale model. Results demonstrate that the statistical parameters of a polychromatic wave may be estimated from the measurement of pressure variation in a buoy with a moonpool.**

Keywords —**Oscillating water column, Prototype design, Wave measurement, Wave spectra.**

I. Introduction

A Number of different methods are used to estimate the sea-sate at a location which may be broadly grouped into three categories: *methods based on measurements taken below the sea-surface*, *methods based on measurements taken on the sea surface* and *methods based on measurements taken above the sea surface* [1]. Examples of the first method include the use of pressure sensors, where the pressure at the sensor is a measure of wave height and inverted echo sounders mounted on the sea-bed. Such systems are suitable for shallow water applications.

Methods which fall into the second category include the use of resistance or capacitance wavestaffs which directly measured the sea surface where structures exist to allow such staffs be deployed and wave rider buoys, where the acceleration of a floating buoy which is assumed to follow the sea surface is measured. The acceleration is doubly integrated to determine the displacement of the buoy, and hence the sea surface elevation. Such buoys may also measure the tilt in two orthogonal directions so that the directional spectra may be measured. Such buoys include the Datawell Waverider range and the SEAWATCH Wavescan Buoy. The third category includes systems which use near–surface measurements by downward-pointing laser, infra-red, radar or acoustic instruments, which may be used if a suitable platform is available, and systems which use measurements taken from from larger distances, such as radar altimeters and satellite altimeters. The advantages and disadvantages of each category are described in [1] and [2].

The work described in this paper has been undertaken as part of an effort to develop a new low-cost, wave powered buoy to measure the local wave regimes to meet the needs of both developers and local authorities, which would fall into the second category above and would be suitable for medium to deep water situations. It is envisioned a number of such low-cost buoys may potentially be deployed at a location to measure the local wave climate both temporally and spatially. The proposed device, christened the Wave-Activated Sensor Power Buoy (WASP) will comprise a floating body with a centre moonpool. The relative motion of the water level in the moonpool to the buoy will pressurise and depressurise the air above the water column. The air flows generated by the change in pressure will, in the final design of the device, be used to drive a bidirectional turbine in the manner of an oscillating water column (OWC), which will be used in conjunction with a generator to recharge an on-board battery pack. Hence, the full-scale WASP would be, in part at least, wave powered, although other sources, such as solar panels may also be employed. For a detailed review of OWC technology, see, for example, [3]. It is intended that, once the WASP has been suitably calibrated, the wave spectrum may be estimated from measurements of the pressure of the air above the water column. Important statistical parameters relating to the sea-state, such as the significant wave height, zero-cross period etc. may then be estimated from the spectral moments of the wave spectrum. Mathematical techniques may be used to determine sea-states from the time series of the air pressure. Such techniques include inverse transfer functions, neural networks and numerical estimators, each of which is currently the

Track: Wave Resource Characterization, Paper ID: 1531.

M. Boland was with the Centre for Renewable Energy at Dundalk IT, Dundalk, Ireland (e-mail: mark@bolandengineering.ie).

T. Kelly is with the Centre for Renewable Energy at Dundalk IT, Dundalk, Ireland (e-mail: kellyt@dkit.com).

R. Carolan is with the Dundalk Institute of Technology, Dundalk, Ireland (e-mail: robert.carolan@dkit.ie).

B. Walsh is with the Dundalk Institute of Technology, Dundalk, Ireland (e-mail: brendan.walsh@dkit.ie).

T. Dooley is with the Dundalk Institute of Technology, Dundalk, Ireland (e-mail: thomas.dooley@dkit.com).

subject of further investigation, once the WASP has been calibrated.

It is proposed to use a modified, off-the-shelf buoy, the Seagull navigation buoy manufactured by JFC Manufacturing Company Ltd., Ireland, for the initial sea trails of the WASP concept. However, before full-scale testing, a campaign of model scale testing was undertaken at a scale of 1:20 in a narrow wave tank located at Dundalk Institute of Technology. This paper outlines the theory used to estimate a sea-state from measurements of the air pressure in a chamber located above the water column in a floating buoy. Next, the 1:20 model is described, before the testing campaign conducted to calibrate the model and validate the measurement process is outlined. Results are then presented to demonstrate that the statistical parameters of a polychromatic wave may indeed be estimated from the measurement of pressure variation in a floating buoy with a moonpool using an inverse transfer function. Finally, an issue with using the inverse transfer function approach is described, as well as proposed improvements to the measurement process.

II. Theory

A number of methods are under investigation to relate the pressure signal in the air chamber above the water column to the incident wave spectrum including inverse transfer functions, neural networks and mathematical estimators. This work focusses on the inverse transfer function method.

Consider the single-input, single output (SISO) system in Figure 1 below.

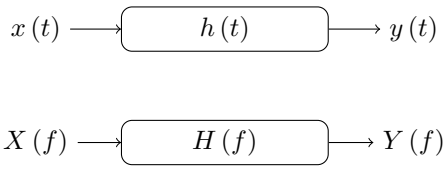

Fig. 1. A single-input/single-output system in the time domain and the frequency domain.

In Figure 1:

$x(t)$	represents the stationary input
$y(t)$	represents the output
$h(\tau)$	represents the impulse response of the system
$X(f)$	represents the Fourier transform of $x(t)$
$Y(f)$	represents the Fourier transform of $y(t)$
$H(f)$	is the frequency-dependent, Fourier transfer function between $X(f)$ and $Y(f)$

$H(f)$ is the Fourier transform of $h(\tau)$.

The two-sided, autospectral density function, $S_{xx}(f)$ for an input time signal $x(t)$ is related to the autospectral density function, $S_{yy}(f)$ for an output signal $y(t)$ by:

$$S_{yy}(f) = |H(f)|^2 S_{xx}(f) \tag{1}$$

Similarly, the two-sided, cross-spectral density function, $S_{xy}(f)$ of the two time signals, $x(t)$ and $y(t)$ are related by:

$$S_{xy}(f) = H(f) S_{xx}(f) \tag{2}$$

In 1 and 2, the frequency may be either positive or negative, and both $S_{yy}(f)$ and $S_{xy}(f)$ are two-sided. In terms of one-sided spectral density functions, which are defined for positive frequencies only, 1 and 2 become:

$$G_{xy}(f) = H(f) G_{xx}(f) \tag{3}$$

$$G_{yy}(f) = |H(f)|^2 G_{xx}(f) \tag{4}$$

where:

$G_{xy}(f)$	is the one-sided cross power spectral density of $x(t)$ and $y(t)$
$G_{xx}(f)$	is the one-sided power spectral density of $x(t)$
$G_{yy}(f)$	is the one-sided power spectral density of $y(t)$

The frequency-dependent transfer function of an SISO system may thus be written:

$$H(f) = \frac{G_{xy}(f)}{G_{xx}(f)} \tag{5}$$

A full treatment of the theory underpinning spectral analysis may be found in, for example, [4].

III. 3-D Model

Froude scaling is used throughout the model construction and testing campaign, hence all dimensions of the model are scaled geometrically [5]. The model was constructed at a scale of 1:20. The scale was chosen based on the physical size of the narrow tank, the range of wave amplitudes and frequencies which may be generated in the narrow tank, and following consideration of the typical wave regimes encountered at the proposed deployment location for the first full-scale prototype, which is to be the 1:4 scale marine test site in Galway Bay, operated by SmartBay [6]. As three-dimensional drawings of the full-scale Seagull where available, it was decided that the 1:20 model would be created using a 3-D printer based on fused filament fabrication. Figure 2 depicts the full-scale Seagull buoy to be used to construct the prototype WASP. The buoy comprises a central structural core of the buoy, which, at full scale, is constructed from 12mm galvanised steel. Four floats, each one quadrant, provide the required buoyancy. At full scale, the floats are constructed in a rotational mould from 10mm polyethylene. One or more polyethylene daymarks may be mounted on the structural core.

A. Structural Core

Initially, the drawing provided by JFC Ltd. were scaled by 1:20 for printing. However, it quickly became apparent that, at a scale of 1:20, the members of the core would be 0.6mm thick, which would be difficult to 3-D print and too fragile to test. To ensure a robust structure for printing and testing, the core wall

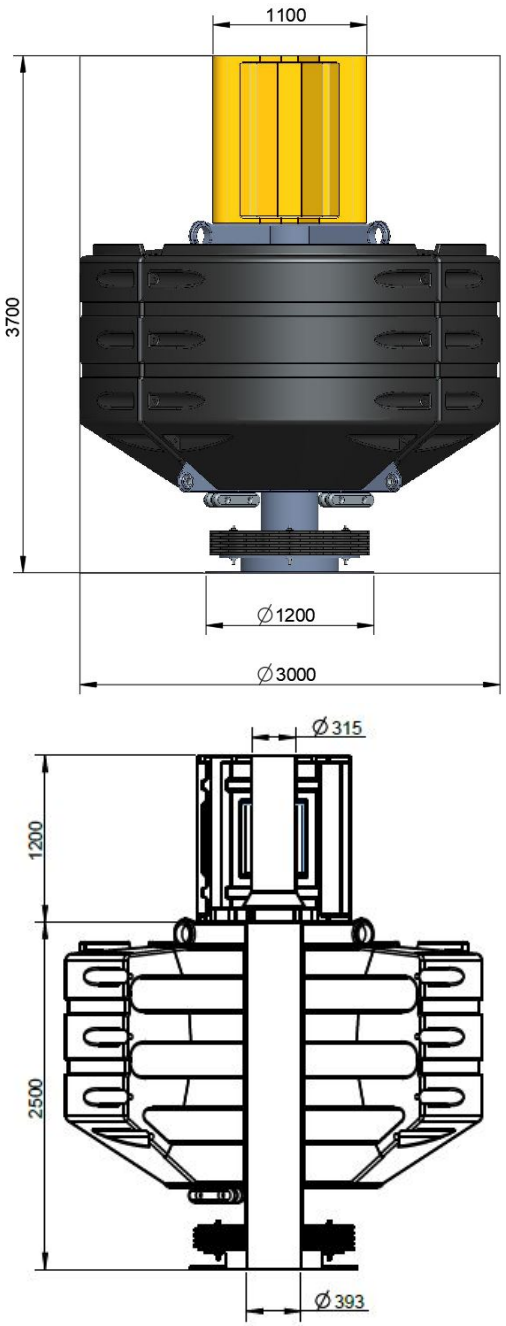

Fig. 2. JFC Seagull SG3000 buoy - (Courtesy of JFC Marine).

thickness was increased to 2.5mm. Figure 3 illustrates the drawing used to print the model core. The nature of the overhangs associated with the core required extensive use of support material during the 3-D printing process. The model buoy was printed using a Leapfrog XEED dual nozzle 3D printer. This allowed the core to be printed in black polylactic acid (PLA) and the support structure in white acrylonitrile butadiene styrene (ABS). The alternative colours and materials allow an easier separation of the support structure from the printed component, nonetheless, considerable time was spent on the subsequent removal of the support material.

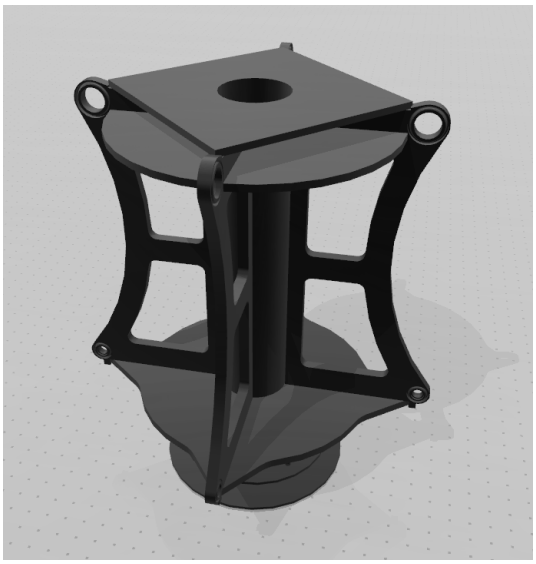

Fig. 3. Drawing of model buoy core for 3-D printing.

B. Floats

The four model floats were printed using a 2 mm side wall and minimal infill. Once printed the floats were sanded, sealed, primed and sprayed to ensure no water penetration and provide sufficient buoyancy during the testing. Figure 4 illustrates the drawing used to print one of the floats. A total of four floats were printed.

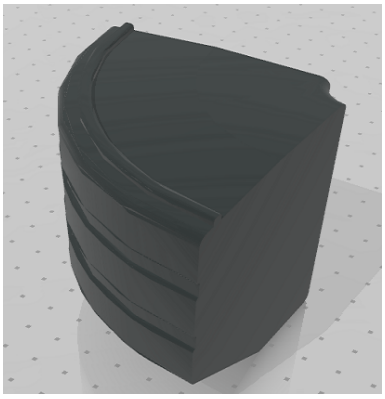

Fig. 4. Drawing of model buoy float for 3-D printing.

C. Daymark

In order to create a tight seal on top of the moonpool, the inside of the daymark was adapted to fit a rubber grommet. A support structure was also created, which was used to hold the pressure sensor in place during testing. Figure 5 illustrates the drawing used to 3-D print the daymark. Once all parts were printed and all support material was removed, the parts were sanded to ensure a good fit, and sealed and primed to ensure water tightness. Figure 6 illustrates the final 3-D model used for testing.

One issue that occurred with the 3-D model arose from the fact that the model structural core was constructed from plastic, unlike the full scale core, which is constructed from steel. Thus, the mass distribution

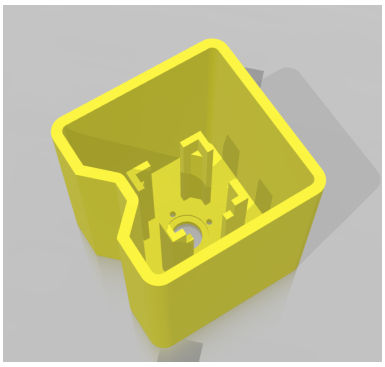

Fig. 5. Drawing of model daymark for 3-D printing.

Fig. 6. 1:20 scale 3-D printed model of the WASP.

of the model buoy was incorrect, which resulted in the buoy pitching excessively in response to an incident wave. To overcome this issue, a weight was suspended below the buoy to lower the centre of gravity.

IV. Testing Campaign

In this section, the choice of wave spectra used to calibrate and then test the model WASP are described. Next, the actual testing process is described.

D. Test Spectra

It is proposed that the first sea trails of a prototype WASP will take place at the SmartBay 1/4 scale marine test site,located off the west coast of Galway, Ireland. The wave regime at the test site has been measured since 2005, using individual Datawell Waverider buoys and the wave climate at the site is well established [7]. The recorded data is freely distributed by the Marine Institute through its request for digital data programme [8]. Figure 7 displays a wave rose of the recorded wave directions and significant wave heights recorded by one of the waveriders buoys at the test site from 2008 and 2018. Zero up-crossing period was also analysed.

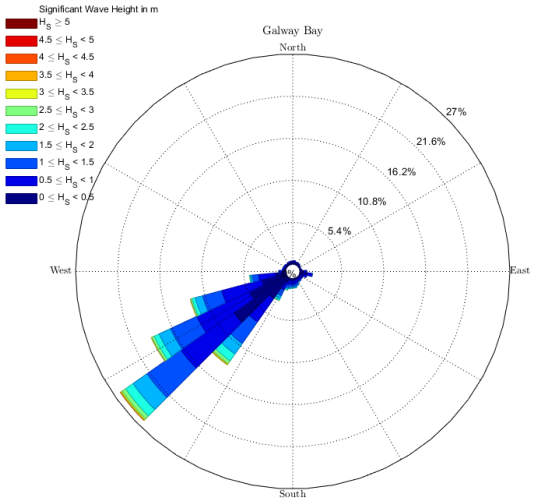

Fig. 7. Wave Rose from the directional waverider buoy at SmartBay, Ireland - (2008 - 2018).

TABLE I
Bretschneider spectra used to test the model WASP

Model-scale H_s (mm)	Model-scale T_z (s)	Full-scale H_s (mm)	Full-scale T_z (s)
84.8	2.23	1696	10
84.4	2.01	1688	9
84.1	1.78	1682	8
84.3	1.55	1686	7
85.1	1.32	1702	6
86.1	1.11	1722	5
84	0.93	1680	4

With the limitations of the wave tank in mind, a range of sea-states were selected to be used throughout testing that reflect the typical sea-states which occur at the SmartBay test site. The theoretical Bretschneider spectra for each selected sea state, based on the significant wave height and zero up-crossing period, was scaled appropriately for testing. For a description of the theoretical parametrised Bretschneider spectrum, see, for example, [9]. Table I lists the wave spectra that were used during the testing at both full scale and model scale. Note that, in accordance with Froude scaling, to obtain the scale equivalent the significant wave height is divided by the scaling factor (here 20), and the zero-crossing period is divided by the square root of the scaling factor. Note the model scale significant wave height is given in millimeters. In all cases, the values of H_s and T_z have been obtained from consideration of the free surface elevation. The periods correspond to full-scale periods of 10 s to 4 s. In each case, the tank was requested to generate a H_s of 75 mm, corresponding to a full-scale H_s of 1.5 m. In practice, the tank created spectra with larger values of H_s close to 1.7m and requires further calibration, this however has no bearing on the results as the estimated spectrum is compared to the recorded and not the requested spectrum.

E. Testing facilities

The 1:20 scale model of the WASP was tested in a narrow wave tank located at the Dundalk Institute of

Technology, Ireland. The tank, which was designed and built by Edinburgh Designs is approximately 18 m in length, 350 mm wide and is filled to a depth of 1 m. At one end of the tank is located a wave absorbing beach proven to absorb on average 98% of incident waves using Goda and Suzuki's method, [10] and at the other end is a wedge-shaped, flap-like wave maker. The tank is capable of generating both monochromatic and polychromatic waves in a frequency range from 0.4 Hz to 1.4 Hz. The pressure of the air above the sealed moonpool of the model is measured using a Honeywell 170PC series differential pressure sensor. Data is acquired and recorded using hardware and software produced by National Instruments. Figure (8) provides a comparison of the measured Bretschnieder spectrum $H_S = 84.8mm$ and $T_Z = 2.23\ sec$ with and without the model in the tank

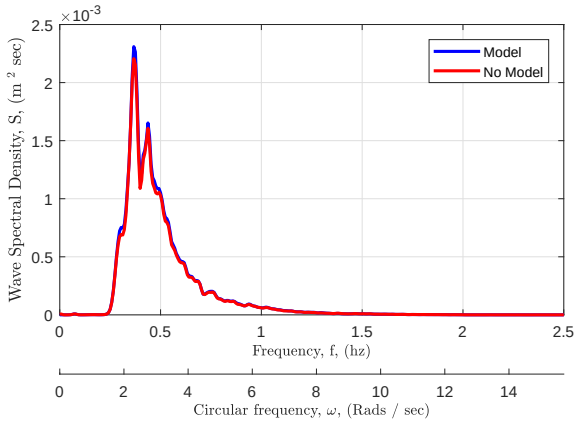

Fig. 8. Comparison of Measured Spectrum with and without the model in the tank, $H_S = 84.8mm$ and Wave Period, $T_Z = 2.33\ sec$.

Figure (9) provides a comparison of the measured Bretschnieder spectrum time series with and without the model in the tank

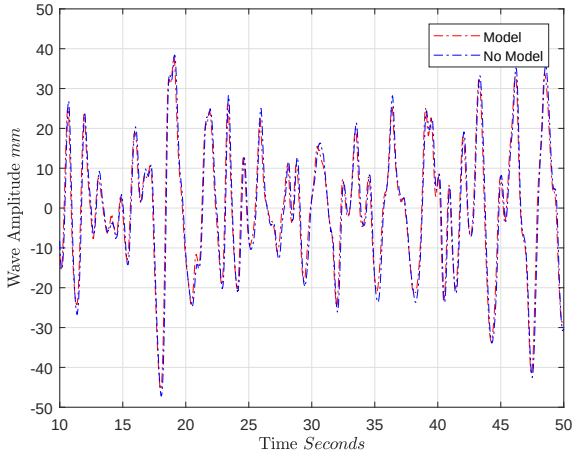

Fig. 9. Comparison of Produced Time Series.

Analysis of Figures (8) & (9) infer that the wave tank can produced a comparable spectrum each time and that the presence of the model has minimal impact.

F. Testing procedure

In order to use the WASP to estimate an incident wave spectrum from the power density spectrum of the time series of the pressure in a chamber of air located above the entrapped water column, it is first necessary to establish the relationship between the pressure spectrum and in the incident wave spectrum. In effect, the WASP must be trained, or calibrated. During the first step of the training process, a Bretschneider spectrum is run in the narrow tank with no model present in the tank for sufficient time to allow the spectrum develop fully (approximately 20 minutes). The free surface elevation is measured throughout the test at a single location using a resistive wave probe, and Welch's method is used to estimate the power density spectrum for the polychromatic wave [11]. Figure 10 illustrates the spectrum generated by the tank estimated using Welch's method, and the theoretical spectrum for a significant wave height of 75 mm and zero-crossing period of 2.33 s (equivalent to 1.5 m and 10 s at full scale), and is representative of the typical output from the narrow tank in response to a requested spectrum.

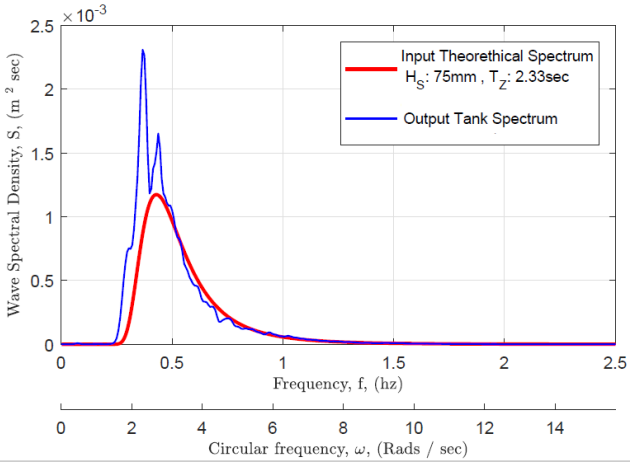

Fig. 10. Spectrum generated by the narrow wave tank v.s theoretical Bretschneider spectrum, H_S = 75 mm and Wave Period, T_Z = 2:33 s.

During the second step of the calibration process, the model is installed in the tank. During the tests discussed herein, a two-point mooring system was simulated using chain and fishing floats. The model draft was set using lead weights. A 176PC14HD2 Honeywell pressure sensor was installed. Once the pressure sensor is installed and the model placed in the tank, the air chamber above the water column is completely sealed. The model was then subjected to the identical Bretschneider spectrum as that illustrated in Figure 10 for sufficient time to all the spectrum fully develop. The pressure in the air above the water column was sampled at 32 Hz throughout the test. It has previously been demonstrated that the narrow wave tank at the Dundalk Institute of Technology is capable of repeatably generating the same polychromatic time series of waves as input to tests separated in time [12]. The power density spectrum of the pressure signal is then estimated, again using Welch's method, and (5) is then used to estimate the frequency dependent

transfer function between the pressure signal and the incident wave elevation. Figure 11 is a photograph of the model WASP in the tank ready for testing. Once the

Fig. 11. Photograph of the completed 3D WASP Model ready for testing.

transfer function has been estimated in this fashion, the wave spectra listed in Table I were run in the absence of the model WASP in order to determine the exact wave spectrum generated for all Bretschneider spectra to be estimated from measurement of the air pressure above the water column of the model. The model was then returned to the tank, and each spectrum re-run while the pressure within the WASP model is recorded. The power density spectrum for each pressure signal is obtained, and the transfer function obtained earlier used to estimate the incident wave spectrum in each case.

V. Results

Figure 12 illustrates the input spectrum that was first used to calibrate the model WASP and establish the relationship between the incident wave power density spectrum and the corresponding pressure power density spectrum. This spectrum had a H_s = 84.8 mm and T_z = 2.23 s. Note that the values for H_s and T_z above were obtained from consideration of the wave spectrum obtained from free surface elevation measurement. Once a wave spectrum is measured, both H_s and T_z may be obtained from the spectral moments. A spectral moment is given by:

$$m_n = \int_0^\infty \omega^n S(\omega)\, dw \tag{6}$$

and $_s$ and T_z may be found by [9]:

$$H_s = 4\sqrt{m_o} \tag{7}$$

$$T_z = \frac{m_1}{m_0} \tag{8}$$

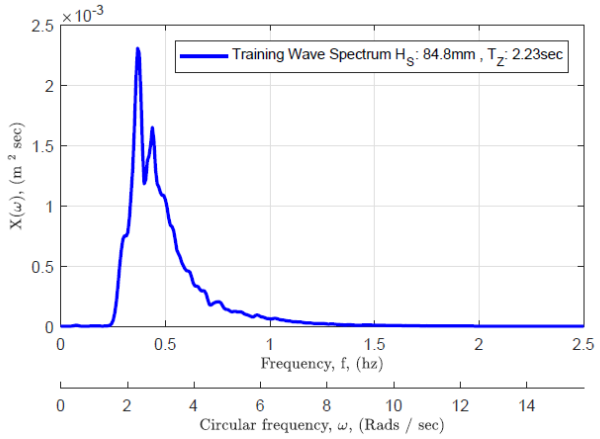

Fig. 12. Incident wave spectrum used to train model WASP, H_S = 84.8 mm and T_z = 2.23s.

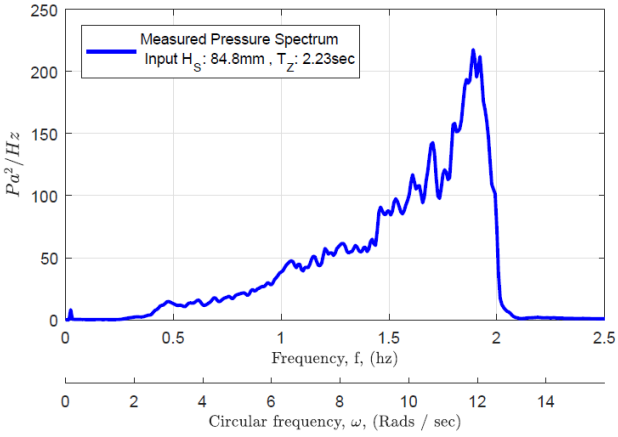

Fig. 13. Pressure Spectrum obtained with an incident wave spectrum of H_S = 84.8 mm, T_z = 2.23s.

Figure 13 illustrates the power density spectrum of the pressure signal recorded during the training run, and Figure 14 illustrates the frequency dependent transfer function between the input wave spectrum and the pressure spectrum obtain by apply (5) to the data in Figures 13 and 12.

Next, to test the transfer function shown in Figure 14, the model was subjected to an incident wave spectrum for a spectrum close to, but not identical, to that for which the transfer function was generated, in this case, a spectrum with a H_s = 88.9 mm and T_z = 2.01 s. The transfer function was used with the pressure spectrum to estimate the incident wave spectrum. Figure 15 illustrates the comparison between the wave spectrum in the absence of a model in the tank, and that predicted by using pressure data from the model WASP with the transfer function in Figure 14.

When spectral moments are determined from the estimated spectrum shown in Figure 15 and used with (7) and (8) to estimate the key spectral parameters, values of H_s = 88.9 and T_z = 2.06, a difference from the corresponding values obtained from measurement of the free surface elevation of approximately 5%.

In order to investigate the viability of using a single

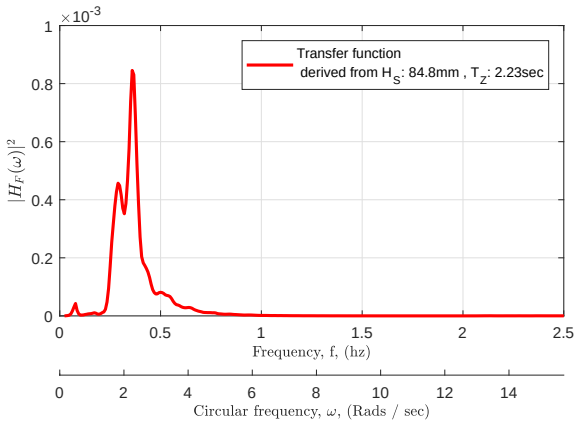

Fig. 14. Transfer function obtained from applying (5) to the data obtained with H_S = 84.8 mm, T_z = 2.23s.

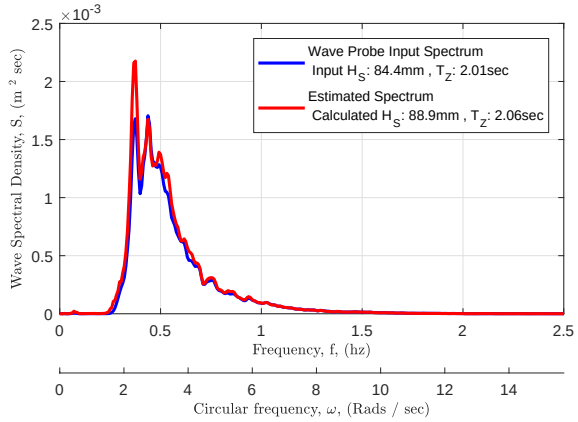

Fig. 15. Comparison between the incident wave spectrum with H_s = 84.5 mm and T_z = 2.01 s and the estimated spectrum using the pressure spectrum and the transfer function illustrated in Figure 14.

transfer function to estimate a range of sea states, the model WASP was then subjected to a series of wave spectral as described in Table I. In each case, the power density spectrum from the pressure signal was used with the transfer function in Figure 14 to estimate the incident wave spectrum. Figure 16 illustrates the comparison between the input wave spectrum and that estimated using the pressure signal as described above for values of H_s = 84.1 mm and T_z = 1.78 s.

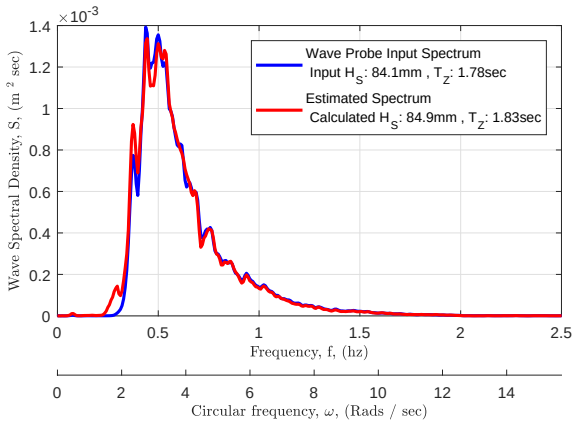

Fig. 16. Comparison between the incident wave spectrum with H_s = 84.1 mm and T_z = 1.78 s and the estimated spectrum using the pressure spectrum and the transfer function illustrated in Figure 14.

For the test illustrated in Figure 16, the estimated values were H_s = 84.9 mm and T_z = 1.83 s. However, while initial results proved very positive, it is possible to see the beginning of an issue in Figure 16. A small peak in the estimated spectrum is visible at a frequency of 0.25 Hz, which is not present in the actual wave spectrum. Figures 17 to 19 show that, as the zero-crossing period decreases from that used in the training spectrum, the anomalous peak at 0.25 Hz grows, and thus increasingly effects the estimated spectral moments and estimated values of H_s and T_z.

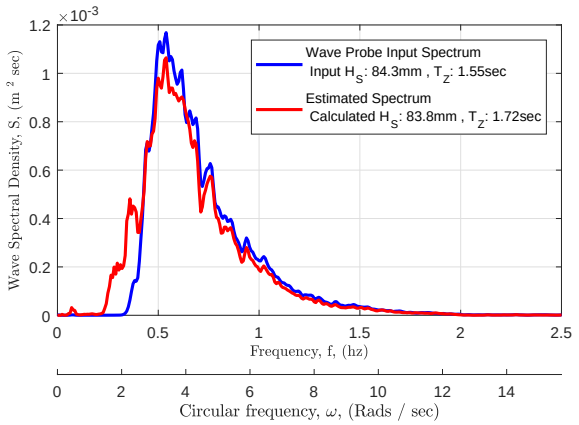

Fig. 17. Comparison between the incident wave spectrum with H_s = 84.3 mm and T_z = 1.55 s and the estimated spectrum using the pressure spectrum and the transfer function illustrated in Figure 14.

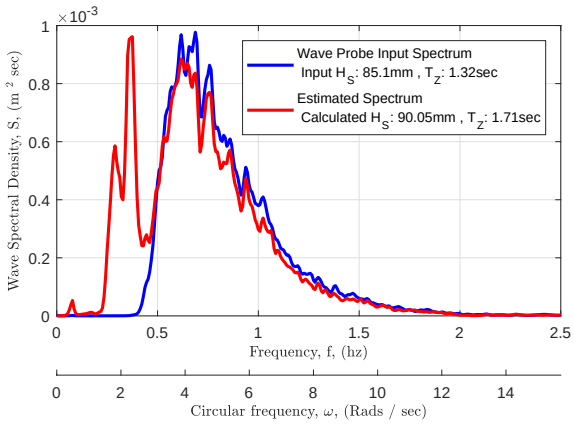

Fig. 18. Comparison between the incident wave spectrum with H_s = 85.1 mm and T_z = 1.32 s and the estimated spectrum using the pressure spectrum and the transfer function illustrated in Figure 14.

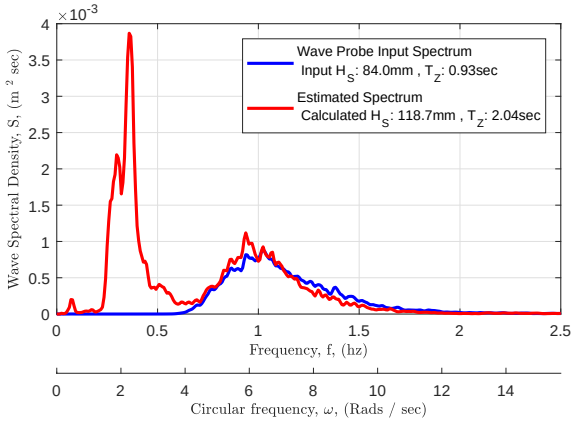

Fig. 19. Comparison between the incident wave spectrum with H_s = 84 mm and T_z = 0.93 s and the estimated spectrum using the pressure spectrum and the transfer function illustrated in Figure 14.

G. Issue with results.

The authors believe the results presented herein, which represent a sample of the results obtained to date, demonstrate that the incident wave spectrum acting on a device such as the WASP can be recovered from the pressure signal by considering the frequency domain transfer function between the power density spectrum of the pressure signal and the incident wave spectrum as described herein. However, clearly an issue does exist. The accuracy of the estimated spectrum as the zero-crossing period decreases clearly decreases in line with the reduction in the amount of energy in the range of 0.25 Hz to 0.4 Hz. In other words, provided the input wave spectrum contains energy in the range of frequencies where the issue arises, the estimated wave spectrum will likely be close to the actual wave spectrum. Conversely, if the incident wave spectrum does not contain much energy at these frequencies, the anomalous peak, which can be seen in Figures 17 to 19, will occur. The authors believe the issue may lie with the very low pressures that are generated in the frequency range where the anomalous peak appears. As can been seen in Figure 13, there is essentially no pressure generated in the air chamber above the moonpool at these frequencies.

Tests have shown that creating a transfer function using data obtained from testing with an incident wave spectrum that does not contain energy in the 0.25 Hz to 0.4 Hz range will not result in the anomalous peak, but as would be expected, will not correctly predict the spectrum when used to estimate wave spectra which do contain energy in the frequency range at issue. A number of approaches are under investigation to address the issue. First and foremost, it is intended that the final WASP device be self-powered, in part using wave energy. Rather than using a sealed OWC chamber, the full-scale device would use the air pressures generated by the water column to drive a Well's (or other) turbine. Thus, it is desirable that the water column and/or the buoy which contains the water column, be excited at all incident wave frequencies likely to be experienced during operation. The Seagull buoy was chosen to form the basis of the initial prototype (and of the model described herein) as it is commercially available at this time. The Seagull design is not, however, optimised for wave power generation. A suitable redesign of the buoy and water column would allow the device to be excited over the full range of frequencies likely to be experienced (and hence measured), and would potentially eliminate this issue.

The use of neural networks to create a black-box model between the incident wave spectrum and the pressure spectrum is also under investigation. Another approach under consideration is the use of estimators based on numerical models of the WASP derived from potential flow to estimate the sea-state from the pressure signal.

VI. Conclusions

The authors believe the work described in this paper indicates that further investigating into the viability of using the pressure signal in a floating OWC to measure a sea-state at larger scales is merited and, it is hoped, this work will lead to a low-cost wave measuring buoy. At this time, and following on from this work, a full-scale prototype of the WASP device has been constructed and is undergoing final tests before deployment in early March 2019 at the SmartBay test facility. Should this test prove successful, future work will focus on low-cost, low-power alternatives to the existing on-board data acquisition and communication systems. Further is is intended that a redesigned buoy be used to explore the use of wave power to power the entire system. However, further work on signal processing remains to be carried out.

ACKNOWLEDGEMENT

The authors would like to acknowledge the JFC Group, Tuam Co. Galway for providing 3-D drawing of, and information on, the Seagull Navigation Buoy that forms the platform of the current WASP design.

The authors would like to further acknowledge the Centre for Renewable Energy at Dundalk IT for unfettered access to the narrow wave tank over a number of days to perform the tests used to produce the results presented herein.

REFERENCES

[1] W. M. Organization, *Guide to Wave Analysis and Forecasting*, ser. Guide to Wave Analysis and Forecasting. Secretariat of the World Meteorological Organization, WMO, 1988.
[2] J. Cruz, *Ocean Wave Energy: Current Status and Future Prespectives*, 1st ed. Berlin: Springer Verlag, 2010.
[3] A. F. O. Falcão and J. C. C. Henriques, "Oscillating-water-column wave energy converters and air turbines: A review," *Renewable Energy*, vol. 85, pp. 1391–1424, 2016.
[4] J. Bendat and A. Piersol, *Engineering Applications of Correlation and Spectral Analysis*. Wiley, 1980.
[5] B. Massey and J. Ward-Smith, *Mechanics of Fluids*. CRC Press:London, UK, 1998.
[6] B. G. Cahill and T. Lewis, "Wave energy resource characterisation of the Atlantic Marine Energy Test Site," *International Journal of Marine Energy*, vol. 1, pp. 3–15, 2013.
[7] B. G. Cahill, *Resource Characterisation of the Galway Bay 1/4 Scale Wave Energy Test Site*. Prepared on behalf of the Sustainable Energy Authority of Ireland., 2012.
[8] Marine Institute. (2019) Home - Marine Institute. [Online]. Available: https://www.marine.ie/Home
[9] S. K. Chakrabarti, *Hydrodynamics of Offshore Structures*. Berlin: Springer Verlag, 1987.
[10] Y. Goda and Y. Suzuki, "Estimation of incident and reflected waves in random wave experiments," *Coastal engineering proceedings*, vol. 1, 01 1976.
[11] P. D. Welch, "The use of fast Fourier transform for the estimation of power spectra: A method based on time averaging over short, modified periodograms," *IEEE Transactions on Audio and Electroacoustics*, vol. 15, pp. 70–73, 1967.
[12] T. Kelly, T. Dooley, and J. V. Ringwood, "Experimental determination of the hydrodynamic parameters of an owc," in *Proceedings of the 12th European Wave and Tidal Energy Conference*, Cork, Ireland, 2017, p. 915.1 – 915.10.